Journal of the European Ceramic Society 44 (2024) 585–594

Contents lists available at ScienceDirect

Journal of the European Ceramic Society

journal homepage: www.elsevier.com/locate/jeurceramsoc

Phase stability of high entropy oxides: A critical review

Martina Fracchia [a,b,*], Mauro Coduri [a,b,*], Paolo Ghigna [a,b], Umberto Anselmi-Tamburini [a,b]

[a] Department of Chemistry, University of Pavia, V.le Taramelli 12, I27100 Pavia, Italy
[b] INSTM, National Inter-University Consortium for Materials Science and Technology, Via G. Giusti 9, 50121 Florence, Italy

ARTICLE INFO

Keywords:
High entropy oxides
Configurational entropy
Phase stability
High entropy ceramics
Solid solution

ABSTRACT

After the discovery of the prototypical high-entropy oxide with formula $Cu_{0.2}Zn_{0.2}Mg_{0.2}Co_{0.2}Ni_{0.2}O$, the research on these materials has shown a dramatic boost. While many studies were devoted to exploring their possible applications, only few addressed the effective reasons behind their stability. The possibility to achieve a single-phase structure is usually hastily attributed to configurational entropy. This resulted in an extensive misuse of the terms "entropy-stabilized oxides" and "high-entropy oxides", often employed as synonyms. However, the effective role of entropy in the stabilization should be demonstrated for each system, and even for $Cu_{0.2}Zn_{0.2}Mg_{0.2}Co_{0.2}Ni_{0.2}O$ it is still under debate. Moreover, many effects concur to the stabilization, *i.e.* the relative concentration, the valence state and the ionic radii of the cations involved. We will here discuss the role of configurational entropy in the phase stability, considering the main classes of crystal structures and providing a guide to critically discern between entropy and non-entropy stabilized oxides.

1. Introduction

In material sciences, doping, *i.e.* the introduction of *small amounts* of foreign atoms in a host structure, is the most extensively used method for changing and engineering the material properties. How small the amount of dopants is, it depends on the class of materials we are interested in. It can be ppm or ppb in classical semiconductors, range in the percent level in alloys, up to tens of percent in ceramics. However, the identification of the host is always possible and easy: in classical chemistry terminology, in these materials we have a solvent and a solute, where the solvent is the component that is present in the largest amount.

This rationale was somehow undermined by the concept of high entropy alloys [1,2], which are formed by mixing nearly equal or relatively large amounts of five or more components (configurational entropy for a mixture of a given number of chemical components is maximum for the equimolar composition). It is quite obvious that in this case the identification of the solvent is almost impossible. High entropy alloys have been extensively studied since nearly three decades, with a noteworthy flourishing in research in the 2010's, as the large value of configurational entropy, which is achieved in these materials, acts as a phase stabilizing term. For example, in a 2004 paper [1], Cantor reported the synthesis of a 20-component alloy containing 5 at% of Mn, Cr, Fe, Co, Ni, Cu, Ag, W, Mo, Nb, Al, Cd, Sn, Pb, Bi, Zn, Ge, Si, Sb, and Mg. In such a system at constant pressure, the Gibbs phase rule would allow for up to 21 phases at equilibrium, but far fewer actually formed. High entropy alloys may have desirable properties such as better strength-to-weight ratios, higher degree of fracture resistance, tensile strength, and corrosion and oxidation resistance than conventional alloys [3–5].

The concept of high entropy was extended to oxides by Rost et al. [6], who in 2015 reported the formation of a single phase solid solution with the rock salt structure with the $Mg_{0.2}Co_{0.2}Ni_{0.2}Cu_{0.2}Zn_{0.2}O$ composition. Since then, several other high entropy ceramics have been reported, including diborides [7,8], chalcogenides [9], silicides [10] and other intermetallics such as half Heusler [11,12]. Moreover, the synthesis of perovskite oxides [13], fluorite oxides [14,15], spinel oxides [16,17] and many others was also described.

Despite this huge effort in the search of new high entropy materials, the basic understanding of these systems is still in its infancy, and several problems are still open. For instance:

1. The "high entropy concept" implies, in principle, a random sampling of the compositional space. However, this is rarely done in the synthesis of these compounds, since chemical intuition and solubility/stability criteria (Hume-Rothery and/or Pauling rules) are rather followed with the aim of synthesizing single-phase materials. This is equivalent to limiting the entire compositional space to a small

* Corresponding authors at: Department of Chemistry, University of Pavia, V.le Taramelli 12, I27100 Pavia, Italy.
E-mail addresses: martina.fracchia@unipv.it (M. Fracchia), mauro.coduri@unipv.it (M. Coduri).

https://doi.org/10.1016/j.jeurceramsoc.2023.09.056
Received 2 August 2023; Received in revised form 13 September 2023; Accepted 21 September 2023
Available online 22 September 2023

volume fraction. For example, high entropy spinels are always prepared from spinel-forming oxides. Configurational entropy in this case definitely acts as a stabilizing term, but it is more likely a bonus rather than the main contribution to the Gibbs free energy.

2. The role of each chemical component in defining the final crystal structure is often underestimated. This point may be better clarified if we consider, as an example, the $Mg_{0.2}Co_{0.2}Ni_{0.2}Cu_{0.2}Zn_{0.2}O$ material, with the rock salt structure. From a thermodynamic point of view, the synthesis of this material can be thought as divided into two steps. In the first step, the three oxides with the rock salt native structure (MgO, CoO and NiO) form an equimolar solid solution. This process is (at least at a good approximation) isenthalpic, and the Gibbs free energy is negative and fully determined by the entropy of mixing. In the second step, monoclinic CuO and hexagonal ZnO dissolve in the previously formed rock salt solid solution. The enthalpy variation for this second process is positive and given by the enthalpies of transition of CuO and ZnO from their ground state crystal structure to the rock salt structure. It is however well known from the equilibrium phase diagrams that the solubility of CuO and ZnO in rock salt oxides can be as high as 20% (molar fraction), which means that the entropy of mixing is large enough to compensate for the positive enthalpy contribution. In this case, it is quite apparent that the rock salt structure acts as an "overall solvent" where oxides with other crystal structures can dissolve [18].
3. Strictly related with the above point is the fact that increasing the number of chemical components while maintaining the constrain of equimolar composition implies that the molar fractions of each of the components are decreasing and therefore the solubility limit of each of the components can be respected independently of the value of the configurational entropy.
4. The weight of configurational entropy in the Gibbs free energy of formation $\Delta_{form}G = \Delta_{form}H\text{-}T\Delta_{form}S$ is linearly dependent of temperature. This implies that solid solutions that are stable at the synthesis temperature can be metastable at room temperature. This is the case of $Mg_{0.2}Co_{0.2}Ni_{0.2}Cu_{0.2}Zn_{0.2}O$, which is known to distort towards a tetragonal structure when heated from RT to *ca.* 250 °C [19].
5. When high entropy ceramics are employed as catalysts or electrodes for lithium ion batteries, where chemical reactivity is desired, the quest for stability may be detrimental rather than beneficial. However, high entropy ceramics often show better performances when compared to the parent materials also in this respect [20–22]. In the science of high entropy materials, this is often related to the so-called "cocktail effect", where inter-element interactions give rise to unexpected behaviour. However, it is not clear if this effect is exclusive to the high entropy materials:[23] it may be argued that the properties of every material critically depend on composition.

In this review, we will critically discuss the role of configurational entropy in the phase stabilization of high entropy oxides (HEO). The aim of this work is to contribute to the solution of the abovementioned problems. For the reader's convenience, we will start our discussion with a detailed calculation of configurational entropy in a solid solution having a generic crystal structure; then, some considerations concerning the terminology used in the science of high entropy materials will follow. We will henceforth review the pertinent aspect concerning the phase stability of high entropy oxides, ordering the discussion by classes of crystal structure.

2. Configurational entropy for a solid solution with *i* components

Some inconsistences are present in the literature concerning the configurational entropy of a generic solid solution with a generic number of components, and several different ways for calculating the configurational entropy are reported [24–26]. This confusion mainly arises as the science of high entropy materials was born in the field of alloys, where the crystal structures are simple and, generally, just one crystallographic site (Wyckoff position) is occupied. The starting point we here propose is to recognize that different Wyckoff positions can be treated independently. We start with the simplest case, *i.e.* when the compositional disorder involves just one Wyckoff position. Let then n_i be the number of atoms of type i in the solid solution. We assume that the Wyckoff position for the i atoms is fully occupied (the case of occupation factor being less than unit is easily derived by letting one of the i being a vacancy). Then, the sum $\sum_i n_i = N$, where N is the total number of Wyckoff positions in the crystal. The number of microstates for the solid solution is given by the number of permutations with repetitions:

$$W = \frac{(\sum_i n_i)!}{\prod_i n_i!} \tag{1}$$

Using Stirling approximation, taking into account that $1/\frac{\sum_i n_i}{n_i}$ is the molar fraction of i, and using Boltzmann's formula for entropy:

$$S_{Config} = k\ln(W) = -k\sum_i n_i \ln\chi_i = -\frac{R}{N_A}\sum_i n_i \ln\chi_i \tag{2}$$

Where N_A is the Avogadro's constant and R is the gas constant. For a mole of Wyckoff positions $\sum_i n_i = N = N_A$ and $n_i = N_A\chi_i$, and then we have:

$$S_{Config} = k\ln(W) = -\frac{R}{N_A}\sum_i n_i \ln\chi_i = -R\sum_i \chi_i \ln\chi_i \tag{3}$$

If we now take into account the more general case when compositional disorder is on more than one Wyckoff position, we need to consider that Wyckoff positions can have different multiplicities. We need to repeat the calculations, using a Wyckoff position with multiplicity p, *i.e.* that can accommodate a number of atoms that is p times as before:

$$W = \frac{(\sum_i pn_i)!}{\prod_i pn_i!} \tag{4}$$

Repeating the calculations as before for a mole of Wyckoff positions we get the same conclusion as Eq.3. Let us now consider a compound having disorder on two different Wyckoff positions, one with multiplicity p and the other with multiplicity q. If Z is the number of unit formula of the compound in the unit cell, then taking a mole of compound means that we have p/Z moles of the first Wyckoff position, and have q/Z moles of the second, and therefore the molar configurational entropy for this solid solution is:

$$S_{Config,TOT} = -R\left(\frac{p}{Z}\sum_i \chi_{i,1}\ln\chi_{i,1} + \frac{q}{Z}\sum_i \chi_{i,2}\ln\chi_{i,2}\right) \tag{5}$$

For example, for a mole of a spinel AB_2O_4, having disorder on both the A and B sites (Wyckoff position 8*a* and 16*d*, respectively), p and q are equal to 8 and 16, respectively, and Z is equal to 8. Therefore:

$$S_{Config,TOT} = -R\left(\sum_i \chi_{i,A}\ln\chi_{i,A} + 2\sum_i \chi_{i,B}\ln\chi_{i,B}\right) \tag{6}$$

The generalization to the case of disorder on any number of Wyckoff positions is straightforward:

$$S_{Config,TOT} = -R\sum_j\left(\frac{p_j}{Z}\sum_i \chi_{i,j}\ln\chi_{i,j}\right) = -R\sum_{i,j}\frac{p_j}{Z}\chi_{i,j}\ln\chi_{i,j} \tag{7}$$

Where the outer summation is on the j Wyckoff positions having multiplicity p_j, and the inner summation is on the i components.

3. Entropy stabilized materials *versus* high entropy materials *versus* compositionally complex materials

It is easy to show that configurational entropy, as calculated in Eq. 7, is maximized when the i components are present in equal amounts, *i.e.* for equimolar mixtures. Then, for the $Mg_{0.2}Co_{0.2}Ni_{0.2}Cu_{0.2}Zn_{0.2}O$ solid solution, $S_{Config} = 1.61R$, while for an equimolar mixture of 4 components $S_{Config} = 1.39R$. There is a general consensus towards the definition of "high entropy materials" as materials for which $S_{Config} > 1.5R$. This is mainly because new properties seem to develop when the entropy is above this limit [1,2]. However, large and positive entropy values are needed only if the enthalpy of mixing is large and positive (endothermic): this is the case of the "entropy stabilized materials" [27]. It can be shown that, in several cases, the enthalpy of mixing is negative (exothermic), and in these cases, the high entropy does not dominate the Gibbs free energy landscape [28]. These "high entropy materials" are evidently not entropy stabilized. Fig. 1 schematically represents this aspect. In particular, Fig. 1a shows how solid solutions can be categorized according to two different characteristics, being the number of components (and the value of configurational entropy thereof) and the effective role of entropy in the phase stabilization.

Moreover, there are several effects, such as clustering at the nanoscale, that can significantly reduce the entropy with respect to the nominal value given in Eq. 7 [29]. All these cases (*i.e.* the negative enthalpy of mixing, or the reduction of configurational entropy with respect to the ideal value) can be included into the so-called "compositionally complex materials" (CCC). Indeed, this term was introduced by Wright et al. [30] to group together high entropy, medium entropy oxides and non-equimolar oxides (see Fig. 1b).

4. High entropy oxides with the rock salt structure

Among the various classes of HEO, those with the rock salt structure are unique as not only they are the first to have been reported, and, consequently, the most investigated, but also as they display special structural properties due to the fact that they always contain Cu^{2+}. Moreover, theoretical calculations, carried out employing both entropy and enthalpy descriptors and considering several M^{2+} cations (*i.e.* Ca, Co, Cu, Fe, Mg, Mn, Ni, Zn), pointed out that the (Cu,Co,Ni,Mg,Zn)O system is the most prone to form a high entropy material bearing a single-phase rock salt structure [31]. Indeed, these calculations show that Ca, Fe and Mn-containing high entropy oxides present unfavorable enthalpy contributions that are far too large to be compensated by configurational entropy, at least at feasible temperatures.

Copper containing oxides are particularly interesting, as Cu^{2+} ions with the d^9 electronic configuration exhibit a strong Jahn-Teller effect, and any regular coordination octahedron around Cu^{2+} would distort giving two long and four short Cu-O distances. This is important, as the displacement of oxides ions will produce additional entropy, and will have an effect on the functional properties of the materials [32]. Local structural distortions in $Mg_{0.2}Co_{0.2}Ni_{0.2}Cu_{0.2}Zn_{0.2}O$ have been deeply investigated, both by means of lattice dynamics [33], and experimentally by X-ray diffraction (XRD) [32] and Extended X-ray Absorption Fine Structure (EXAFS) [34]. It can be demonstrated that no other cation in $Mg_{0.2}Co_{0.2}Ni_{0.2}Cu_{0.2}Zn_{0.2}O$ has such an effect [33]. Moreover, the Jahn-Teller distortion drives a cubic-to-tetragonal phase distortion [19,32], which is evidenced by large deviations in the width of some diffraction peaks with respect to the ideal case. This effect critically depends on the amount of copper in the solid solutions, and it is demonstrated that it is larger when the fraction of copper increases up to 0.24.

Moreover, $Mg_{0.2}Co_{0.2}Ni_{0.2}Cu_{0.2}Zn_{0.2}O$ has a prominent role in the field of HEO as it is believed to possess all the properties that are characteristic of entropy stabilized materials: reversible phase transition, formation of a crystal structure distinct from that of at least two end-members, positive enthalpy of formation. However, a recent study demonstrates that the phase behavior of the five-component rock salt is not markedly different than that of four or three-component copper-containing rock salt solid solutions having the same ratio of native rock salt oxides (MgO, CoO, and NiO) [18]. Fig. 2a, b report the XRD and transmission electron microscopy (TEM) for binary $Ni_{0.8}Cu_{0.2}O$, three-cation $Ni_{0.6}Cu_{0.2}Zn_{0.2}O$ and four-cation $Ni_{0.4}Co_{0.2}Cu_{0.2}Zn_{0.2}O$, compared to $Mg_{0.2}Co_{0.2}Ni_{0.2}Cu_{0.2}Zn_{0.2}O$. All the solid solutions were obtained as single phase rock salt with homogeneous cation distribution down to the nanometer scale, and all of them are thermodynamically stable until down to 850 °C. These results implicate that conventional solubility limits have a prominent role: in general, dissolution processes in the solid state are endothermic and therefore entropy driven. This casts doubts on the role of configurational entropy as the leading term of the Gibbs free energy of formation of these solid solutions. Moreover, this study underlines that the presence of a reversible phase transition from single phase to multiphase in high entropy oxides is a necessary but not sufficient criterion to corroborate the stabilization by configurational entropy.

The problem of phase stability is evidently crucial when applications, such as in the field of electrochemistry or catalysis, are concerned [22,

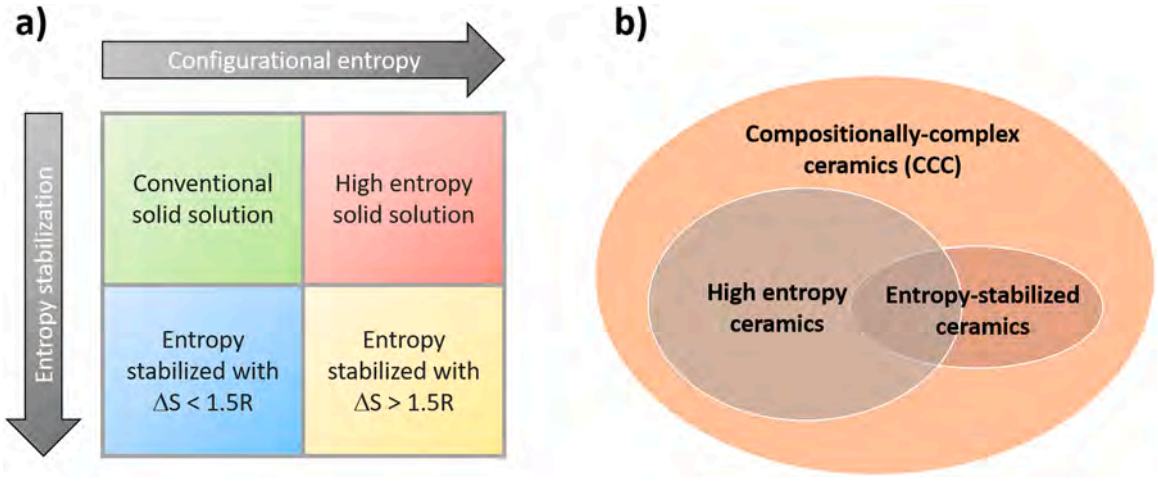

Fig. 1. : a) Scheme representing how solid solutions can be categorized according to the number of components (leading therefore to a higher configurational entropy) and the presence/absence of entropy stabilization. Copyright 2023 American Chemical Society b) Scheme of compositionally-complex ceramics (CCC), that include either medium-entropy and high-entropy ceramics. Entropy-stabilized ceramics are a small subgroup of the CCC.
(a) Adapted with permission from Reference [28]. (b) Adapted from Reference [30] Copyright(2023), with permission from Elsevier.

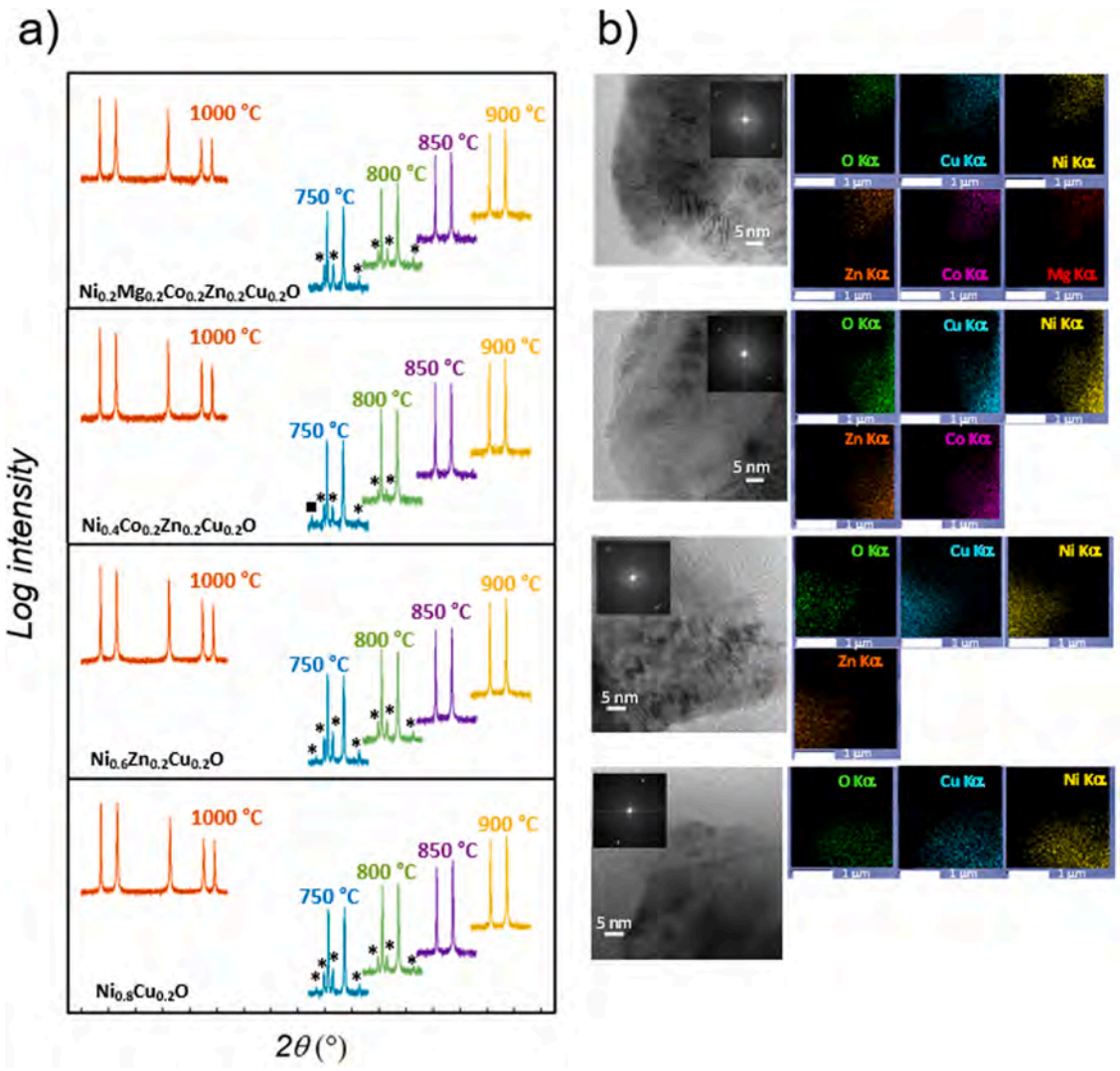

Fig. 2. : a) Powder diffraction patterns for the five-, four-, three- and two-component solid solutions quenched from 1000 °C to RT (red lines). The solid solutions were heated to 900, 850, 800 and 750 °C, and quenched to RT. Asterisks and squares mark the diffraction peaks of CuO tenorite and spinel phases, respectively. b) High-resolution transmission electron microscopy (TEM) with corresponding fast Fourier Transform (FFT) and energy-dispersive spectroscopy (EDS) maps for all the elements present. Instrumental magnification: 400,000 × . Copyright The Authors, some rights reserved; exclusive licensee Springer Nature. Distributed under a creative Commons Attribution License 4.0 (CC BY) https://creativecommons.org/licenses/by/4.0/.
Figure adapted with permission from ref [18].

35–37]. This is particularly true in the case of HEO anodes for Li ion batteries [35,38], where it is claimed that the cations act synergically in determining superior performances compared to simple oxides [20]. Mechanistic studies by means of operando X-ray absorption spectroscopy (XAS) demonstrated a collapse of the rock salt structure upon lithiation, and an irreversible redox mechanism, where the reversible capacity was ascribed to the alloying/dealloying reaction typical of anodes such as ZnO and MgO [39]. However, more recently, it has been shown that the original rock salt structure state can be recovered from the post-lithiation polyphase in ball mill prepared HEO [40].

5. High entropy oxides with the fluorite and related structures (bixbyite, pyrochlores)

One of the first evidences of the formation of high entropy oxides bearing the fluorite structure was reported in 2017 by Djenadic et al. [14]., where equiatomic single phase materials containing up to seven rare-earth cations were successfully synthesized. The rare-earth metals involved were Ce, La, Nd, Pr, Sm, Y and Gd. It was observed that, for this system, the presence of cerium is mandatory to obtain a single phase structure, which can be achieved notwithstanding the number of elements involved. Indeed, equiatomic composition with 3, 4, 5 and 6 metal cations led to a pure fluorite structure (space group *Fm*-3*m*), while the 7-component system showed a decreased symmetry compatible with the formation of a single phase bixbyite (space group *Ia*-3). It should be noted that, out of all the considered elements, only Ce and Pr oxides are usually stable in the fluorite structure, respectively as CeO_2 and Pr_6O_{11}. However, it is well-known from literature that all the other cations show extensive solubility in CeO_2. In order to investigate on a possible role of entropy in the stabilization of these systems, the as-synthesized 5-component oxide $(Ce,La,Pr,Sm,Y)O_{2-\delta}$ was heat-treated at two different temperatures, lower than the one employed for the synthesis (1050 °C). While at 750 °C no phase separation was observed, at 1000 °C additional peaks appeared in the XRD pattern, indicative of a symmetry lowering from *Fm*-3*m* to *Ia*-3. In any case, no reversible entropy-driven transition from single phase to multiphase, expected in case of an entropy-stabilized system, was detected, thus allowing to conclude that the type of elements, rather than the amount of configurational entropy, are the main responsible for the structure stabilization.

The first high entropy fluorite containing both transition and rare-

earth cations was reported in 2018 [15]. The authors successfully synthesized eight pure oxides, seven of which having a configurational entropy larger than 1.5 *R*, being the minimum threshold generally adopted to define a high entropy material. However, no additional data on the phase stability at different temperatures were provided. Conversely, in the same year, Chen et al. claimed the synthesis of an entropy stabilized fluorite with composition $(Ce_{0.2}Zr_{0.2}Hf_{0.2}Sn_{0.2}Ti_{0.2})O_2$ [29], though with a small amount of secondary phase evidenced by XRD and energy dispersive spectroscopy (EDS). As mentioned above, a fundamental prerequisite for a system to be entropy stabilized is that not all the oxide precursors should share the same crystal structure. In this case, as in most cases for high entropy fluorite systems, this criterion is satisfied. Indeed, while CeO_2, ZrO_2 and HfO_2 are usually found in the fluorite structure, SnO_2 and TiO_2 are mostly stable as rutile. Another criterion regards the presence of a reversible transition from single phase to multiphase upon cooling. The temperature for the synthesis was 1500 °C. Calcinations at lower temperatures showed the reversible formation of new XRD signals, attributed to the formation of a second phase. A similar result was reported later by Spiridigliozzi et al. with the composition $(Ce_{0.2}Zr_{0.2}Y_{0.2}La_{0.2}Gd_{0.2})O_{1.7}$ [41]. Again, a treatment to temperatures lower than the one employed for the synthesis led to the segregation of a secondary phase that was attributed to bixbyite (possibly Gd_2O_3 or La/Y doped-Gd_2O_3). Nevertheless, we here note that the reversibility from a higher-temperature single phase to a lower-temperature multiphase systems is undoubtedly a mandatory condition for entropy stabilization, though *per se* not sufficient. For instance, the role of solubility equilibria should be carefully taken into consideration before imputing the phase stabilization to the sole large configurational entropy value [18,28].

It is also worth noting that several medium entropy fluorites, with less than five cations or with compositions far from the equimolar, have also been successfully synthesized at the same temperature [30], suggesting that entropy may not be the main factor governing the stabilization of fluorite-related structures. This fact, coupled to the extensive chemical variability hosted in these systems, that makes it difficult to widely explore all the possible elemental combinations and, consequently, to easily determine the stabilizing factors, prompted the researchers to search for rationalized criteria to predict *a priori* the formation of a single phase fluorite. Velasco et al. employed a high-throughput method, integrating the synthesis of 106 samples, their characterization with XRD, Raman and UV-Vis spectroscopy, and machine learning, to explore the system $(Ce_{0.2}Pr_{0.2}La_{0.2}Sm_{0.2}Y_{0.2})O_{2-\delta}$ [42]. Of all samples, 91 contained three or more elements. Fig. 3 shows the isothermal multicomponent phase diagram at 750 °C comprising the 91 compositions (for details on the interpretation of these plots, the reader is referred to Ref [42]).

Interestingly, only five samples showed the presence of multiple phases, while 76 samples crystallized as single phase fluorite and 10 as single phase bixbyite. The high-throughput screening showed that not only Ce^{4+}, but also Pr, being in a mixed +3 and +4 oxidation state, can lead to phase purity, even in absence of cerium. Moreover, it was noticed that samples with lower configurational entropy (ranging from 1.1 to 1.6 *R* in the present study) can be also stabilized as single phase as long as a +4 or a mixed +3 ,+4 cation is present.

Regarding the possibility to obtain either a fluorite or a bixbyite single phase compound, Spiridigliozzi et al. proposed a predictive model based on the cationic radii [43]. In particular, the authors found that the final structure is linked to the mismatch between the size of the cations, expressed as the standard deviation *s* of the involved cationic distribution. If $s > 0.095$, a single phase oxide with the fluorite structure is obtained. When *s* is lower than 0.095, the sample crystallizes as a single phase bixbyite. A mixture of the two phases is found in correspondence of the threshold value. This empirical rule was obtained after investigating 18 compositions, all containing in equimolar ratio Ce and other four elements among Zr, Y, Yb, La, Gd, Sm, Nd, Pr, Er and Ho. It was later demonstrated that this predictor is not strictly related to the presence of Ce and that is still valid when the configurational entropy is lower than 1.5 *R*, *i.e.* for Zr-containing compositions such as $(Zr_{0.2}La_{0.2}Pr_{0.2}Sm_{0.2}Y_{0.2})O_{2-\delta}$, $(Zr_{0.2}La_{0.2}Tb_{0.2}Sm_{0.2}Y_{0.2})O_{2-\delta}$ and $(Zr_{0.25}La_{0.25}Sm_{0.25}Y_{0.25})O_{2-\delta}$ [44]. The same compositions with Sn or Tb

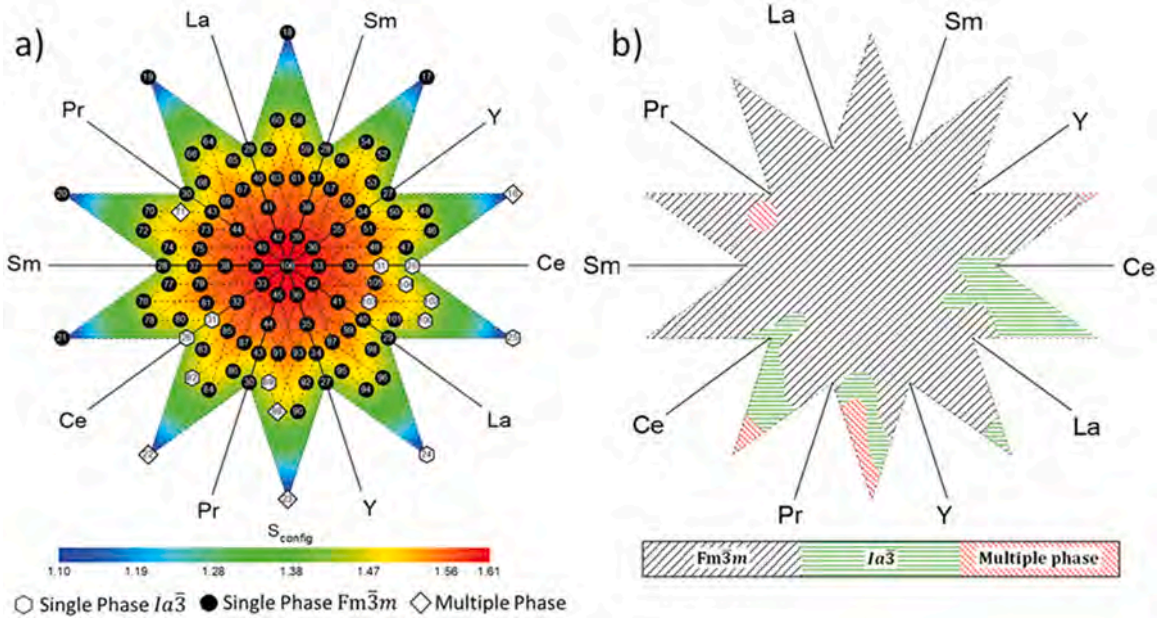

Fig. 3. : Isothermal phase diagrams at 750 °C for 91 oxides, highlighting which of the oxides yields a single or a multiple phase. a) Isothermal multicomponent phase diagram at 750 °C comprising 91 compositions for the chemical deviations from the HEO system $(Ce_{0.2}Pr_{0.2}La_{0.2}Sm_{0.2}Y_{0.2})O_{2-\delta}$. The symbols at the respective compositions show the single or multiple phase nature of the samples. The contour color map relates the configurational entropy Sconfig. b) Isothermal crystallographic phase map obtained for the chemical space of 91 oxides. Details on how to interpret these phase diagrams can be found in Ref [42].
Figure reproduced with permission from ref [42].

replacing Ce or Zr did not result into pure phases, pointing towards the fact that at least one cation with oxidation state +4 and a certain affinity towards a fluorite-related structure is necessary for the stabilization. Moreover, $(Ce_{0.2}La_{0.2}Pr_{0.2}Sm_{0.2}Y_{0.2})O_{2-\delta}$ and $(Zr_{0.2}La_{0.2}Pr_{0.2}Sm_{0.2}Y_{0.2})O_{2-\delta}$, while both pure as fluorites when synthesized at 750 °C, show a different behaviour upon treatment at high temperature; the first promptly forms bixbyite, expected in case of oxygen vacancies ordering [14], while for the second composition this phase transformation is suppressed. This clearly evidences that the individual role of each cation in the structure stabilization can never be neglected.

Another class of materials closely related to fluorites is represented by the pyrochlores, having general formula $A_2B_2O_7$, where A sites are rare-earth, alkaline or alkaline-earth cations and B sites are transition or post-transition cations. The structural stability of the pyrochlores structure strictly depends on the ratio between the average ionic radius of A and B cations (r_A/r_B), according to the criterion proposed by Subramanian [45]. If r_A/r_B is comprised between 1.46 and 1.78, a pyrochlore structure is formed. If r_A/r_B is lower than 1.46, the formation of a defect fluorite structure is favoured, while for values larger than 1.78 a single cubic phase is no more obtained. It has been widely demonstrated that this rule is fully valid also for high entropy pyrochlore structures. The first compositions obtained presented five rare-earth cations in the A site and Zr in the B site, *e.g.* $(La_{0.2}Ce_{0.2}Nd_{0.2}Sm_{0.2}Eu_{0.2})Zr_2O_7$ [46] and $(La_{0.2}Nd_{0.2}Sm_{0.2}Eu_{0.2}Gd_{0.2})Zr_2O_7$ [47], or a progressive number of rare-earth elements (from 1 to 7 among Gd, Eu, Sm, Nd, La, Dy, Ho) in the A site [48]. Analogously, compositions with one cation in the A site and five elements in the B site were reported, namely $Nd_2(Ta_{0.2}Sc_{0.2}Sn_{0.2}Hf_{0.2}Zr_{0.2})_2O_7$ and $Nd_2(Ti_{0.2}Nb_{0.2}Sn_{0.2}Hf_{0.2}Zr_{0.2})_2O_7$ [49]. Pitike et al. employed first-principle calculations, based on DFT, to predict the formation of pyrochlores with La^{3+} or Nd^{3+} on the A site, and five cations in the B site, pre-selected on the basis of their ionic radius and valence state among Hf, Nb, Sc, Sn, Ta, Ti, Zr [50]. The use of proper enthalpy and entropy descriptors allowed a screening of promising compositions, out of which two La^{3+}- and three Nd^{3+} - containing pyrochlores were successfully synthesized as single-phase. Moreover, Monte Carlo simulations were employed to estimate the secondary phase composition as a function of temperature and oxygen partial pressure. The family of compositionally complex pyrochlores was finally extended by introducing multiple cations not only in the A site but also in the B site (*i.e.* Zr, Hf, Sn, Ti) and encompassing both high and medium entropy compositions [51]. Teng et al. synthesized 37 different equiatomic compositions, including 30 high entropy pyrochlore oxides and 7 high entropy fluorite oxides, 33 of which having a single phase structure, confirming in all cases the validity of the Subramanian criterion [52]. It was observed by EDS that cations Gd^{3+}, Eu^{3+}, Sm^{3+}, Nd^{3+}, La^{3+}, Dy^{3+}, Ho^{3+} and Ti^{4+}, Zr^{4+}, Sn^{4+}, Hf^{4+} are homogenously and randomly distributed. The secondary phases were found to be mainly due to Ce^{4+} and Nb^{5+}. In fact, the first has an ionic radius much larger than the other B site cations, while the second has an oxidation state different than +4 . This work, along with the previous ones, point out that, similarly to fluorites, the pyrochlores also present a vast compositional and chemical flexibility, where the phase stabilization is mainly governed by the ionic radii (in particular the r_A/r_B ratio and the mismatch between the ionic radii of cations occupying the same site) and the valence of each cation. To the best of our knowledge, only in one case the stabilization of the pyrochlore was specifically attributed to configurational entropy. Vayer et al. synthesized $Dy_2(Ti_{0.2}Zr_{0.2}Hf_{0.2}Ge_{0.2}Sn_{0.2})_2O_7$ at 1600 °C, obtaining a pure pyrochlore, and subsequently heat-treated the sample at 1400 °C [53]. This resulted into a phase segregation among the cations of the B site, with one phase mainly containing Ge and two other phases containing all the five cations. This single phase to multiphase transition was attributed to entropy stabilization, with the enthalpic penalty induced by Ge, being the only cation that does not form a single phase cubic pyrochlore with Dy.

6. High entropy oxides with the α-PbO_2 structure

The α-PbO_2 structure is particularly relevant to the problem of the phase stability of high entropy oxides, as the four component (Ti,Zr,Hf,Sn)O_2 solid solution [54] is a good candidate for being entropy stabilized [28]. This material, which may be defined as "medium entropy", meets both the requirements of i) crystal structure different from that of any of the end members and ii) positive formation enthalpy. Indeed, at room temperature TiO_2 and SnO_2 are stable in the rutile structure (tetragonal, space group $P4_2/mnm$), ZrO_2 and HfO_2 as baddeleyite (monoclinic, space group $P2_1/c$), while (Ti,Zr,Hf,Sn)O_2 is finally orthorhombic (space group *Pbcn*). Fig. 4a shows the XRD pattern of the sample obtained at 1400 °C, demonstrating the formation of a single-phase material. To test reversibility, this sample was then treated from room temperature to 1200 °C, measuring the thermal conductivity and acquiring XRD patterns at significant temperatures. The thermal conductivity showed an increase until 900 °C, compatible with a demixing of the starting components. Above this temperature, a decrease in the thermal conductivity was instead observed, suggesting the progressive formation of the orthorhombic single-phase solid solution. Indeed, this hypothesis is confirmed by XRD, displayed in Fig. 4b, where it can be observed that the peaks related to the single phase orthorhombic (Ti,Zr,Hf,Sn)O_2 start to reappear above 1200 °C, along with the progressive disappearance of those related to the raw materials.

Very recently, attempts have been made to synthesize the five-component (Ti,Zr,Hf,Sn,Ge)O_2, which is predicted to display the same crystal structure and which has the potentiality to be a truly high entropy material (in the sense of entropy stabilized). However, up to now they are yet not successful [55].

7. High entropy oxides with the perovskite structure

Most of the experimental studies on high entropy perovskites are focused on single selected compositions dedicated to some specific applications, such as thermoelectrics [56], proton conductors [57] or catalysts [58]. Works explicitly discussing the possible role of configurational entropy in the stabilization of the perovskite phases are scarce [13,59], while others [60,61] tackle a systematic approach to unveil all possible combinations of components based on their valence distribution. We have first to point out that these studies refer to different kinds of perovskites (Sarkar et al. on trivalent A and B cations, the other studies on perovskites with A^{2+} and B^{4+}) and different synthetic routes, particularly concerning the synthesis temperature, the duration of the reaction and the cooling rate. This makes difficult to compare the results and to ascertain the common structural features characterising high entropy perovskites.

The first report on high entropy perovskites is provided by Jiang et al. [13]. They produced 13 candidates of high entropy perovskites, placing either Ba^{2+} or Sr^{2+} on the A site, while the B site is shared by five cations in equimolar ratio, selected to have Goldschmidt's tolerance factors [62] ranging from 0.95 to 1.05. We here remind that the tolerance factor is calculated from the ionic radii through the following equation:

$$t = \frac{r_A + r_X}{\sqrt{2}(r_B + r_X)} \tag{8}$$

Where r_A is the radius of the A cation, r_B is the radius of the B cation and r_X is the radius of the anion.

The single oxide powders were ball-milled, compressed as pellets, heated at 1300, 1400 and 1500 °C (duration not provided) and cooled in the furnace. With only one exception, single phase perovskites form only when the tolerance factor lies within 0.98 and 1.02, while no correlation is observed with respect to the atomic-size difference (δ), defined as:

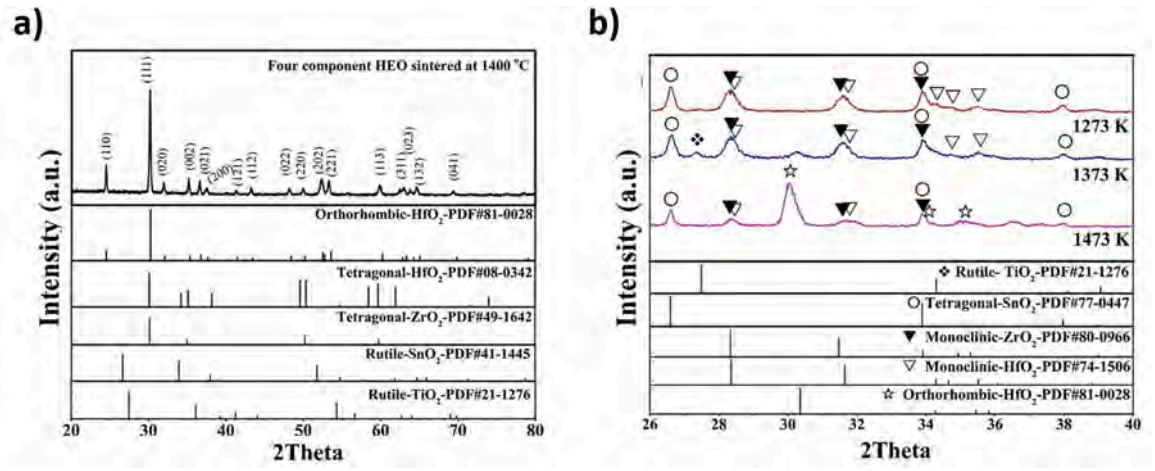

Fig. 4. : a) XRD pattern of (Ti,Zr,Hf,Sn)O_2 sintered for 4 h at 1400 °C, compared to some reference patterns. b) XRD patterns of the samples obtained after thermal conductivity test under the temperature of 1273, 1373, and 1473 K.
(a) Figure adapted from ref [54]. (b) Copyright(2023), with permission from Elsevier.

$$\partial(r_B) = \sum_{I=1}^{5} C_i \left(1 - \frac{r_i}{\sum_{I=1}^{5} C_i r_i}\right) \tag{9}$$

Where C_i and r_i are the molar fraction and radius of the *i*-the ion.

All the produced single phase perovskites have the prototype cubic structure. Entropy is considered to be able to play a role in the stabilization of a single phase for two reasons. First, moving from a 4- to a 5-cation oxide (adding Mn to Zr, Sn, Ti and Hf at the B site), leads to a single perovskite phase, which does not form in the absence of Mn. This is clearly consistent with an increase of configurational entropy from 1.39 R to 1.60 R. The stabilizing effect of entropy occurs, however, assuming that no further enthalpy contribution is added by increasing the molar fraction of each cation from 0.20 to 0.25. Second, the coexistence of Ba and Sr on the A site, when equimolar Zr, Hf, Sn, Nb and Ti occupy the B site, leads a single perovskite phase which is stable in a wider temperature range (at 1400 °C and 1500 °C) compared to when only Ba (stable at 1300 °C) or only Sr (stable at 1500 °C) are present. In addition, the mixed Sr-Ba A site leads to a tolerance factor equal to 1.0, which is already a factor stabilizing the single perovskite phase, while in the case only Sr or Ba occupy the A site, *t* becomes 0.97 and 1.03, respectively. This is a geometrical contribution which can help stabilizing the single phase, regardless of entropy. On the other hand, the fact that more compositions are single phase at 1300 °C, but secondary phases are found at higher temperature, is not consistent with entropy stabilization.

Sarkar et al. investigated different high entropy perovskites combining five trivalent cations on the A and/or the B sites [59]. The perovskites were prepared by spray pyrolysis, followed by a 2-hour thermal treatment at 1200 °C without quenching. Only few compositions form a single perovskite phase, all of them being orthorhombic. The closer the tolerance factor *t* to 1.0, the lesser the orthorhombic strain. It is proposed that the high entropy perovskites are stabilized by entropy because: i) the $(5A_{0.2})MnO_3$ system undergoes a reversible decomposition into more orthorhombic perovskite phases while cooling below a critical temperature of about 900 °C; this temperature behavior recalls that of the prototype rock salt HEO observed by Rost et al. [6]. However, we point out that the demixing of the rock salt phase occurs with the segregation of the CuO parent oxide. In the present case, the demixing leads to the formation of a multiphase system composed of different perovskites with the same crystal structure and likely a complex distribution of more cations; ii) a 10-cation system $(5A_{0.2})(5B_{0.2})O_3$ forms a single phase and shows no evidence of decomposition upon temperature, while $(5A_{0.2})BO_3$ and $A(5B_{0.2})O_3$ systems do not even form single phases. The formation of a single phase in the presence of 10 cations is deemed as a proof of entropy stabilization.

The above investigations were limited to equimolar combinations of cations, sharing in principle the same valence state. In the search for new stable high entropy perovskites, Tang et al. [60]. and Ma et al. [61]. proposed a systematic approach looking for all combinations of cations with different valence granting electroneutrality for the ABO_3 perovskite system. Among many possible combinations of cations and valences, Tang et al. limited their study to $Ba(5B_{0.2})O_3$ perovskites, providing a set of 12 valence combinations of B cations from +2 to +6 valence states and equimolar ratio. Once defined the valence of each cation, the perovskite compositions were designed in order to keep the tolerance factor *t* as close to 1.0 as possible. The specimens were fired for 6 h at different temperatures (1200–1600 °C) after mixing the single oxide powder *via* ball milling. They noticed that $0.97 < t \leq 1.03$ not only gives cubic perovskites, but also, with only one exception, allows to obtain a single phase high entropy perovskite. In addition, they found no correlation between the formation of superstructure peaks, index of a lower symmetry perovskite, and the cation-size difference. A relation is rather observed with respect to the valence mismatch, calculated according to:

$$\partial(V_B) = \sum_{I=1}^{5} C_i \left(1 - \frac{V_i}{\sum_{I=1}^{5} C_i V_i}\right) \tag{10}$$

Where C_i and V_i are the molar fraction and valence of the *i*-the ion.

Ma et al. continued the work by Tang et al., exploring non-equimolar compositions, still focusing on perovskite with $A=Ba^{2+}$ and 5 cations sharing the B site. Among 86 combinations, 12 of them show configurational entropy above 1.5 *R*. It seems that in non-equimolar compounds no correlation occurs between the formation of a single phase and the tolerance factor, while the correlation between valence mismatch and superstructure distortion is confirmed.

8. High entropy oxides with the spinel structure

This class of high entropy oxides received large attention in the literature [16,63–66]. This is unsurprising, given the number of technological applications involving oxides presenting this crystal structure. Particular attention has been given to the use of these oxides as electrodic materials for Li- and Na-based batteries [67,68]. The spinel structure involves two different crystallographic cationic sites, one

tetrahedral and one octahedral, plus one position for oxygen atoms. The tetrahedral sites are generally occupied by a divalent cation, while the octahedral from a trivalent cation. The presence of two cationic sublattices allows the possibility of site inversion, with the divalent cations occupying the octahedral site and the trivalent cations occupying the tetrahedral sites. Furthermore, some spinels present the possibility of deviation from the ideal stoichiometry. Cation site vacancies are produced together with charge-compensating oxygen vacancies in such a case. The possibility of these crystallographic disorders allows a further contribution to the configurational entropy of the material.

The majority of literature related to HEO presenting this crystal structure is focused mainly on the possibility of creating materials with a large number of cations placed on the two available crystallographic sites to enhance or modify the functional properties of the material [16,66,69]. Limited attention has been paid to phase stability. The spinel structure is robust enough to host many different kinds of bivalent and trivalent cations without losing stability and giving rise to decomposition processes. As a result, in this class of materials, the phenomena representing the hallmark of entropy stabilization, such as modification in phase stability resulting from an increase in temperature or in the number of components, have never been reported.

Some insights on the role played by the configurational entropy on the phase stability of these materials have been recently presented by Riley et al. [70]. The authors have been investigating the phase stability of several spinels presenting substoichiometry of the bivalent cations. Cationic substoichiometric spinels produce both cationic and anionic vacancies that contribute to the configurational entropy of the materials but also reduce their phase stability. When treated at temperatures below 800 °C these substoichiometric spinels evidenced the formation of secondary oxide phases. However, single phase spinels can be obtained when the same compositions are treated at 900 or 950 °C and quenched, a behavior similar to the one reported in HEO with different crystal structures. An increase in the number of divalent cations from one to four increased the stability of such substoichiometric phases, allowing to obtain monophasic materials without any segregation of divalent oxides even after treatment of 800 °C. This influence of the number of components has been considered similar to the one presented by the rock salts HEO, considered prototypical of this class of materials. These results suggested that an increase in the number of components can indeed increase the stability even in this class of HEO.

Several authors evidenced that an increase in the number of cations may influence the crystallographic site occupancy [16,64,71,72]. In several instances, in fact, it has been reported that the introduction of many different cations on the two available crystallographic sites produces complex distributions resulting in partial or total inversion [16,73]. Sarkar et al. pointed out that, for the system with nominal formula $(Co_{0.2}Cr_{0.2}Fe_{0.2}Mn_{0.2}Ni_{0.2})_3O_4$, the cations are not randomly distributed in the octahedral and tetrahedral sites, but are rather distributed as to give the lowest configurational entropy allowed by the given composition in a spinel structure [73]. This clearly indicates that enthalpy factors, in particular the crystal field stabilization energy, play a leading role over configurational entropy in determining the effective cation distribution.

The reported results, however, are still very preliminary and refer only to a few specific compositions. More investigations are required to be able to draw some general considerations regarding this aspect.

9. Conclusions

After an in-depth digression on how to calculate the configurational entropy in solid solutions with a generic crystal structure, and a clarification regarding the terminology employed in the science of high entropy materials, the factors contributing to the phase stability of the main oxide crystal structures have been examined. High entropy spinels, fluorites, perovskites and pyrochlores present a vast compositional and chemical flexibility, with robust structures able to host many different elements. In these cases, phase stabilization can be achieved by a sapient choice of cations, considering the interplay between their relative concentration, the valence state and the ionic radii. For fluorites, pyrochlores and perovskites, empirical rules can be followed to predict *a priori* the effective formation of the desired crystal structure. It can be concluded that, overall, configurational entropy does not seem to have a major contribution in the phase stabilization for these systems. We shall also recall here that entropy stabilization implies that the compositional space is sampled randomly, and this is usually not done in the studies reported in the present review: indeed, spinel, perovskite and fluorite high entropy materials are usually prepared from spinel, perovskite and fluorite structure forming oxides.

A more intriguing case surely regards the prototypical high entropy oxide $Cu_{0.2}Zn_{0.2}Mg_{0.2}Co_{0.2}Ni_{0.2}O$. Considering the Gibbs energy of formation at constant T and p for a solid solution, $\Delta_{for}G = \Delta_{mix}H - T\Delta_{mix}S$, if $\Delta_{mix}H$ is large and positive, the term $-T\Delta_{mix}S$ is large and negative only at high temperature. This mere fact, while explaining the high temperatures usually used in the synthesis of these materials, leads to the immediate conclusion that entropy stabilization requires metastability at room temperature. Indeed, reversible demixing with CuO segregation in $Cu_{0.2}Zn_{0.2}Mg_{0.2}Co_{0.2}Ni_{0.2}O$ has been widely assumed as a proof of entropy stabilization. However, more recent studies demonstrated that the behaviour of a three-component rock salt solid solution, having the same ratio of native rock salt oxides (MgO, CoO, and NiO) with respect to the non-native ones (ZnO and CuO), is exactly the same of the five-component solid solution. This seems to indicate that conventional solubility limits, rather than a true entropy stabilization, play the leading role in determining the stability of the $Cu_{0.2}Zn_{0.2}Mg_{0.2}Co_{0.2}Ni_{0.2}O$ HEO. Finally, we shall recall also the emblematic case of the $(Ti,Zr,Hf,Sn)O_2$ medium entropy oxide with the α-PbO_2 structure, with a crystallographic structure different from that of any end member. To the best of our knowledge, this represents a unique case and may indeed be stabilized by entropy. A similar high entropy oxide (with more than 5 cations) sharing this same structure has not been successfully synthesized yet.

The growing interest in this new class of materials has led to a dramatic boost in the synthesis of new compositions bearing several crystal structures. Alongside, high-throughput procedures are rapidly developing, allowing to synthesize tens, if not hundreds, of samples in a limited amount of time. Assessing the factors governing phase stability in the different classes of crystal structures is mandatory to guide the discovery of new pure-phase high entropy materials. As a future outlook, this information, coming from both chemical knowledge and matured experience, can provide a solid input for theoretical calculations / machine learning techniques, allowing for a rational screening in the vast possible compositional space. This information needs to be coupled with a variety of local and long-range probes, to get a better understanding of the role of entropy in stabilizing the structure and on stability. The possibilities of these materials are possibly tremendous, and the present research has just opened the gate towards the discovery of new materials with engineered properties.

Declaration of Competing Interest

The authors declare that they have no known competing financial interests or personal relationships that could have appeared to influence the work reported in this paper.

Acknowledgments

The authors acknowledge support from the Ministero dell'Università e della Ricerca (MUR) and the University of Pavia through the program "Dipartimenti di Eccellenza 2023–2027". M.F. acknowledges funding from the program "L'Oréal Italia per le Donne e la Scienza".

References

[1] B. Cantor, I.T.H. Chang, P. Knight, A.J.B. Vincent, Microstructural development in equiatomic multicomponent alloys, Mater. Sci. Eng. A. 375–377 (2004) 213–218, https://doi.org/10.1016/j.msea.2003.10.257.

[2] J.W. Yeh, S.K. Chen, S.J. Lin, J.Y. Gan, T.S. Chin, T.T. Shun, C.H. Tsau, S.Y. Chang, Nanostructured high-entropy alloys with multiple principal elements: Novel alloy design concepts and outcomes, Adv. Eng. Mater. 6 (2004) 299–303, https://doi.org/10.1002/adem.200300567.

[3] D. Raabe, C.C. Tasan, H. Springer, M. Bausch, From high-entropy alloys to high-entropy steels, Steel Res. Int. 86 (2015) 1127–1138, https://doi.org/10.1002/srin.201500133.

[4] Z. Li, S. Zhao, R.O. Ritchie, M.A. Meyers, Mechanical properties of high-entropy alloys with emphasis on face-centered cubic alloys, Prog. Mater. Sci. 102 (2019) 296–345, https://doi.org/10.1016/j.pmatsci.2018.12.003.

[5] B. Gludovatz, A. Hohenwarter, D. Catoor, E.H. Chang, E.P. George, R.O. Ritchie, A fracture-resistant high-entropy alloy for cryogenic applications, Science 345 (80-.) (2014) 1153–1158, https://doi.org/10.1126/science.1254581.

[6] C.M. Rost, E. Sachet, T. Borman, A. Moballegh, E.C. Dickey, D. Hou, J.L. Jones, S. Curtarolo, J. Maria, Entropy-stabilized oxides, Nat. Commun. 6 (2015) 1–8, https://doi.org/10.1038/ncomms9485.

[7] J. Gild, Y. Zhang, T. Harrington, S. Jiang, T. Hu, M.C. Quinn, W.M. Mellor, N. Zhou, K. Vecchio, J. Luo, High-entropy metal diborides: a new class of high-entropy materials and a new type of ultrahigh temperature ceramics, Sci. Rep. 6 (2016) 2–11, https://doi.org/10.1038/srep37946.

[8] F. Monteverde, F. Saraga, M. Gaboardi, J.R. Plaisier, Compositional pathways and anisotropic thermal expansion of high-entropy transition metal diborides, J. Eur. Ceram. Soc. 41 (2021) 6255–6266, https://doi.org/10.1016/j.jeurceramsoc.2021.05.053.

[9] B. Jiang, Y. Yu, J. Cui, X. Liu, L. Xie, J. Liao, Q. Zhang, Y. Huang, S. Ning, B. Jia, B. Zhu, S. Bai, L. Chen, S.J. Pennycook, J. He, High-entropy-stabilized chalcogenides with high thermoelectric performance, Science 371 (80-.) (2021) 830–834, https://doi.org/10.1126/science.abe1292.

[10] J. Gild, J. Braun, K. Kaufmann, E. Marin, T. Harrington, P. Hopkins, K. Vecchio, J. Luo, A high-entropy silicide: (Mo0.2Nb0.2Ta0.2Ti0.2W0.2)Si2, J. Mater. 5 (2019) 337–343, https://doi.org/10.1016/j.jmat.2019.03.002.

[11] K. Chen, R. Zhang, J.W.G. Bos, M.J. Reece, Synthesis and thermoelectric properties of high-entropy half-Heusler MFe1−xCoxSb (M = equimolar Ti, Zr, Hf, V, Nb, Ta), J. Alloy. Compd. 892 (2022), https://doi.org/10.1016/j.jallcom.2021.162045.

[12] A. Karati, M. Nagini, S. Ghosh, R. Shabadi, K.G. Pradeep, R.C. Mallik, B.S. Murty, U.V. Varadaraju, Ti 2 NiCoSnSb - a new half-Heusler type high-entropy alloy showing simultaneous increase in Seebeck coefficient and electrical conductivity for thermoelectric applications, Sci. Rep. 9 (2019) 1–12, https://doi.org/10.1038/s41598-019-41818-6.

[13] S. Jiang, T. Hu, J. Gild, N. Zhou, J. Nie, M. Qin, T. Harrington, K. Vecchio, J. Luo, A new class of high-entropy perovskite oxides, Scr. Mater. 142 (2018) 116–120, https://doi.org/10.1016/j.scriptamat.2017.08.040.

[14] R. Djenadic, A. Sarkar, O. Clemens, C. Loho, M. Botros, V.S.K. Chakravadhanula, C. Kübel, S.S. Bhattacharya, A.S. Gandhi, H. Hahn, Multicomponent equiatomic rare earth oxides, Mater. Res. Lett. 5 (2017) 102–109, https://doi.org/10.1080/21663831.2016.1220433.

[15] J. Gild, M. Samiee, J.L. Braun, T. Harrington, H. Vega, P.E. Hopkins, K. Vecchio, J. Luo, High-entropy fluorite oxides, J. Eur. Ceram. Soc. 38 (2018) 3578–3584, https://doi.org/10.1016/j.jeurceramsoc.2018.04.010.

[16] M. Fracchia, M. Manzoli, U. Anselmi-Tamburini, P. Ghigna, A new eight-cation inverse high entropy spinel with large configurational entropy in both tetrahedral and octahedral sites: Synthesis and cation distribution by X-ray absorption spectroscopy, Scr. Mater. 188 (2020) 26–31, https://doi.org/10.1016/j.scriptamat.2020.07.002.

[17] J. Dąbrowa, M. Stygar, A. Mikuła, A. Knapik, K. Mroczka, W. Tejchman, M. Danielewski, M. Martin, Synthesis and microstructure of the (Co,Cr,Fe,Mn,Ni)3O4 high entropy oxide characterized by spinel structure, Mater. Lett. 216 (2018) 32–36, https://doi.org/10.1016/j.matlet.2017.12.148.

[18] M. Fracchia, M. Coduri, M. Manzoli, P. Ghigna, U.A. Tamburini, Is configurational entropy the main stabilizing term in rock-salt Mg0.2Co0.2Ni0.2Cu0.2Zn0.2O high entropy oxide? Nat. Commun. 13 (2022) 1–4, https://doi.org/10.1038/s41467-022-30674-0.

[19] M. Fracchia, P. Ghigna, T. Pozzi, U. Anselmi Tamburini, V. Colombo, L. Braglia, P. Torelli, Stabilization by configurational entropy of the Cu(II) active site during CO oxidation on Mg 0.2 Co 0.2 Ni 0.2 Cu 0.2 Zn 0.2 O, J. Phys. Chem. Lett. 11 (2020) 3589–3593, https://doi.org/10.1021/acs.jpclett.0c00602.

[20] K. Wang, W. Hua, X. Huang, D. Stenzel, J. Wang, Z. Ding, Y. Cui, Q. Wang, H. Ehrenberg, B. Breitung, C. Kübel, X. Mu, Synergy of cations in high entropy oxide lithium ion battery anode, Nat. Commun. 14 (2023) 1–9, https://doi.org/10.1038/s41467-023-37034-6.

[21] M. Fracchia, D. Callegari, M. Coduri, U. Anselmi-Tamburini, M. Manzoli, E. Quartarone, P. Ghigna, Electrochemical performance of high and medium entropy oxides for lithium batteries, Front. Energy Res. 10 (2022) 1–9, https://doi.org/10.3389/fenrg.2022.883206.

[22] A. Sarkar, L. Velasco, D. Wang, Q. Wang, G. Talasila, L. de Biasi, C. Kübel, T. Brezesinski, S.S. Bhattacharya, H. Hahn, B. Breitung, High entropy oxides for reversible energy storage, Nat. Commun. 9 (2018), https://doi.org/10.1038/s41467-018-05774-5.

[23] E.J. Pickering, N.G. Jones, High-entropy alloys: a critical assessment of their founding principles and future prospects, Int. Mater. Rev. 61 (2016) 183–202, https://doi.org/10.1080/09506608.2016.1180020.

[24] D.B. Miracle, O.N. Senkov, A critical review of high entropy alloys and related concepts, Acta Mater. 122 (2017) 448–511, https://doi.org/10.1016/j.actamat.2016.08.081.

[25] A. Sarkar, B. Breitung, H. Hahn, High entropy oxides: The role of entropy, enthalpy and synergy, Scr. Mater. 187 (2020) 43–48, https://doi.org/10.1016/j.scriptamat.2020.05.019.

[26] O.F. Dippo, K.S. Vecchio, A universal configurational entropy metric for high-entropy materials, Scr. Mater. 201 (2021), 113974, https://doi.org/10.1016/j.scriptamat.2021.113974.

[27] S.J. McCormack, A. Navrotsky, Thermodynamics of high entropy oxides, Acta Mater. 202 (2021) 1–21, https://doi.org/10.1016/j.actamat.2020.10.043.

[28] S.S. Aamlid, M. Oudah, J. Rottler, A.M. Hallas, Understanding the role of entropy in high entropy oxides, J. Am. Chem. Soc. 145 (2023) 5991–6006, https://doi.org/10.1021/jacs.2c11608.

[29] K. Chen, X. Pei, L. Tang, H. Cheng, Z. Li, C. Li, X. Zhang, L. An, A five-component entropy-stabilized fluorite oxide, J. Eur. Ceram. Soc. 38 (2018) 4161–4164, https://doi.org/10.1016/j.jeurceramsoc.2018.04.063.

[30] A.J. Wright, Q. Wang, C. Huang, A. Nieto, R. Chen, J. Luo, From high-entropy ceramics to compositionally-complex ceramics: A case study of fluorite oxides, J. Eur. Ceram. Soc. 40 (2020) 2120–2129, https://doi.org/10.1016/j.jeurceramsoc.2020.01.015.

[31] K.C. Pitike, S. Kc, M. Eisenbach, C.A. Bridges, V.R. Cooper, Predicting the phase stability of multicomponent high-entropy compounds, Chem. Mater. 32 (2020) 7507–7515, https://doi.org/10.1021/acs.chemmater.0c02702.

[32] D. Berardan, A.K. Meena, S. Franger, C. Herrero, N. Dragoe, Controlled Jahn-Teller distortion in (MgCoNiCuZn)O-based high entropy oxides, J. Alloy. Compd. 704 (2017) 693–700, https://doi.org/10.1016/j.jallcom.2017.02.070.

[33] G. Anand, A.P. Wynn, C.M. Handley, C.L. Freeman, Phase stability and distortion in high-entropy oxides, Acta Mater. 146 (2018) 119–125, https://doi.org/10.1016/j.actamat.2017.12.037.

[34] C.M. Rost, Z. Rak, D.W. Brenner, J.P. Maria, Local structure of the MgxNixCoxCuxZnxO(x=0.2) entropy-stabilized oxide: An EXAFS study, J. Am. Ceram. Soc. 100 (2017) 2732–2738, https://doi.org/10.1111/jace.14756.

[35] A. Sarkar, Q. Wang, A. Schiele, M.R. Chellali, S.S. Bhattacharya, D. Wang, T. Brezesinski, H. Hahn, L. Velasco, B. Breitung, High-entropy oxides: fundamental aspects and electrochemical properties, Adv. Mater. 31 (2019), https://doi.org/10.1002/adma.201806236.

[36] F. Tavani, M. Fracchia, A. Tofoni, L. Braglia, A. Jouve, S. Morandi, M. Manzoli, P. Torelli, P. Ghigna, P. D'Angelo, Structural and mechanistic insights into low-temperature CO oxidation over a prototypical high entropy oxide by Cu L-edge operando soft X-ray absorption spectroscopy, Phys. Chem. Chem. Phys. 23 (2021) 26575–26584, https://doi.org/10.1039/d1cp03946f.

[37] S.H. Albedwawi, A. AlJaberi, G.N. Haidemenopoulos, K. Polychronopoulou, High entropy oxides-exploring a paradigm of promising catalysts: A review, Mater. Des. 202 (2021), 109534, https://doi.org/10.1016/j.matdes.2021.109534.

[38] Q. Wang, A. Sarkar, Z. Li, Y. Lu, L. Velasco, S.S. Bhattacharya, T. Brezesinski, H. Hahn, B. Breitung, High entropy oxides as anode material for Li-ion battery applications: A practical approach, Electrochem. Commun. 100 (2019) 121–125, https://doi.org/10.1016/j.elecom.2019.02.001.

[39] P. Ghigna, L. Airoldi, M. Fracchia, D. Callegari, U. Anselmi-Tamburini, P. D'angelo, N. Pianta, R. Ruffo, G. Cibin, D.O. De Souza, E. Quartarone, Lithiation mechanism in high-entropy oxides as anode materials for Li-ion batteries: an operando XAS study, ACS Appl. Mater. Interfaces 12 (2020) 50344–50354, https://doi.org/10.1021/acsami.0c13161.

[40] L. Su, J. Ren, T. Lu, K. Chen, J. Ouyang, Y. Zhang, X. Zhu, L. Wang, H. Min, W. Luo, Z. Sun, Q. Zhang, Y. Wu, L. Sun, L. Mai, F. Xu, Deciphering structural origins of highly reversible lithium storage in high entropy oxides with in situ transmission electron microscopy, Adv. Mater. 2205751 (2023) 1–14, https://doi.org/10.1002/adma.202205751.

[41] L. Spiridigliozzi, C. Ferone, R. Cioffi, G. Accardo, D. Frattini, G. Dell'Agli, Entropy-stabilized oxides owning fluorite structure obtained by hydrothermal treatment, Mater. (Basel) 13 (2020) 1–12, https://doi.org/10.3390/ma13030558.

[42] L. Velasco, J.S. Castillo, M.V. Kante, J.J. Olaya, P. Friederich, H. Hahn, Phase–property diagrams for multicomponent oxide systems toward materials libraries, Adv. Mater. 33 (2021), https://doi.org/10.1002/adma.202102301.

[43] L. Spiridigliozzi, C. Ferone, R. Cioffi, G. Dell'Agli, A simple and effective predictor to design novel fluorite-structured High Entropy Oxides (HEOs), Acta Mater. 202 (2021) 181–189, https://doi.org/10.1016/j.actamat.2020.10.061.

[44] A. Sarkar, P.K. Mannava, L. Velasco, C. Das, B. Breitung, S.S. Bhattacharya, R. Kruk, H. Hahn, Determining role of individual cations in high entropy oxides: Structure and reversible tuning of optical properties, Scr. Mater. 207 (2022), 114273, https://doi.org/10.1016/j.scriptamat.2021.114273.

[45] M.A. Subramanian, G. Aravamudan, G.V.S. Rao, Oxide pyrochlores: a review, Prog. Solid. St. Chem. 15 (1983) 55–143.

[46] Z. Zhao, H. Xiang, Journal of Materials Science & Technology, J. Mater. Sci. Technol. 35 (2019) 2647–2651, https://doi.org/10.1016/j.jmst.2019.05.054.

[47] F. Li, L. Zhou, J.X. Liu, Y. Liang, G.J. Zhang, High-entropy pyrochlores with low thermal conductivity for thermal barrier coating materials, J. Adv. Ceram. 8 (2019) 576–582, https://doi.org/10.1007/s40145-019-0342-4.

[48] Z. Teng, L. Zhu, Y. Tan, S. Zeng, Y. Xia, Y. Wang, H. Zhang, Synthesis and structures of high-entropy pyrochlore oxides, J. Eur. Ceram. Soc. 40 (2020) 1639–1643, https://doi.org/10.1016/j.jeurceramsoc.2019.12.008.

[49] B. Jiang, C.A. Bridges, R.R. Unocic, K.C. Pitike, V.R. Cooper, Y. Zhang, D. Lin, K. Page, Probing the Local Site Disorder and Distortion in Pyrochlore High-Entropy Oxides, (2021). ⟨https://doi.org/10.1021/jacs.0c10739⟩.

[50] K.C. Pitike, A. Macias, M. Eisenbach, C.A. Bridges, V.R. Cooper, Computationally accelerated discovery of high entropy pyrochlore oxides, Chem. Mater. 34 (2022) 1459–1472, https://doi.org/10.1021/acs.chemmater.1c02361.
[51] A.J. Wright, Q. Wang, S. Ko, K. Man, R. Chen, Size disorder as a descriptor for predicting re duce d thermal conductivity in medium- and high-entropy pyrochlore oxides (Scripta Materialia), Scr. Mater. 181 (2020) 76–81, https://doi.org/10.1016/j.scriptamat.2020.02.011.
[52] Z. Teng, Y. Tan, S. Zeng, Y. Meng, C. Chen, X. Han, H. Zhang, Preparation and phase evolution of high-entropy oxides A2B2O7 with multiple elements at A and B sites, J. Eur. Ceram. Soc. 41 (2021) 3614–3620, https://doi.org/10.1016/j.jeurceramsoc.2021.01.013.
[53] D. Ti, Z. Hf, G. Sn, F. Vayer, C. Decorse, D. Bérardan, N. Dragoe, New entropy-stabilized oxide with pyrochlore structure_ Dy2(Ti0.2Zr0.2Hf0.2Ge0.2Sn0.2)2O7, J. Alloy. Compd. 883 (2021), 160773, https://doi.org/10.1016/j.jallcom.2021.160773.
[54] J. He, Z. Li, Y. Liu, A four-component entropy-stabilized orthorhombic oxide, Mater. Lett. 299 (2021), 130082, https://doi.org/10.1016/j.matlet.2021.130082.
[55] S.S. Aamlid, G.H.J. Johnstone, S. Mugiraneza, M. Oudah, J. Rottler, A.M. Hallas, Phase stability of entropy stabilized oxides with the α-PbO2 structure, Commun. Mater. 4 (1) (2023) 11, https://doi.org/10.1038/s43246-023-00372-5.
[56] T. Maiti, R. Banerjee, S. Chatterjee, M. Ranjan, T. Bhattacharya, S. Mukherjee, S. S. Jana, A. Dwivedi, High-entropy perovskites: An emergent class of oxide thermoelectrics with ultralow thermal conductivity, ACS Sustain. Chem. Eng. 8 (2020) 17022–17032, https://doi.org/10.1021/acssuschemeng.0c03849.
[57] R. Guo, T. He, High-entropy perovskite electrolyte for protonic ceramic fuel cells operating below 600 °C, ACS Mater. Lett. 4 (2022) 1646–1652, https://doi.org/10.1021/acsmaterialslett.2c00542.
[58] D. Chen, S. Nie, L. Wu, X. Zheng, S. Du, X. Duan, Q. Niu, P. Zhang, S. Dai, Metal-tannin coordination assembly route to nanostructured high-entropy oxide perovskites with abundant defects, Chem. Mater. 34 (2022) 1746–1755, https://doi.org/10.1021/acs.chemmater.1c03930.
[59] A. Sarkar, R. Djenadic, D. Wang, C. Hein, R. Kautenburger, O. Clemens, H. Hahn, Rare earth and transition metal based entropy stabilised perovskite type oxides, J. Eur. Ceram. Soc. 38 (2018) 2318–2327, https://doi.org/10.1016/j.jeurceramsoc.2017.12.058.
[60] L. Tang, Z. Li, K. Chen, C. Li, X. Zhang, L. An, High-entropy oxides based on valence combinations: design and practice, J. Am. Ceram. Soc. 104 (2021) 1953–1958, https://doi.org/10.1111/jace.17659.
[61] J. Ma, K. Chen, C. Li, X. Zhang, L. An, High-entropy stoichiometric perovskite oxides based on valence combinations, Ceram. Int. 47 (2021) 24348–24352, https://doi.org/10.1016/j.ceramint.2021.05.148.
[62] V. Goldschmidt, Die Gesetze der Krystallochemie, Naturwissenschaffen 14 (1926) 477–485.
[63] Y. Gao, Y. Liu, H. Yu, D. Zou, High-entropy oxides for catalysis: Status and perspectives, Appl. Catal. A Gen. 631 (2022), 118478, https://doi.org/10.1016/j.apcata.2022.118478.
[64] G.H.J. Johnstone, M.U. González-Rivas, K.M. Taddei, R. Sutarto, G.A. Sawatzky, R. J. Green, M. Oudah, A.M. Hallas, Entropy engineering and tunable magnetic order in the spinel high-entropy oxide, J. Am. Chem. Soc. 144 (2022) 20590–20600, https://doi.org/10.1021/jacs.2c06768.
[65] R.R. Katzbaer, F.M. dos Santos Vieira, I. Dabo, Z. Mao, R.E. Schaak, Band gap narrowing in a high-entropy spinel oxide semiconductor for enhanced oxygen evolution catalysis, J. Am. Chem. Soc. 145 (2023) 6753–6761, https://doi.org/10.1021/jacs.2c12887.
[66] M. Coduri, M. Fracchia, M. Guerrini, C. Dejoie, P. Ghigna, U.A. Tamburini, Novel In-based high entropy spinel oxides with tunable lattice parameter, J. Eur. Ceram. Soc. 43 (2023) 2728–2739, https://doi.org/10.1016/j.jeurceramsoc.2022.12.047.
[67] S.H. Chung, Y.H. Wu, Y.H. Tseng, T.X. Nguyen, J.M. Ting, High entropy oxide (CrMnFeNiMg)3O4 with large compositional space shows long-term stability as cathode in lithium-sulfur batteries, ChemSusChem 16 (2023), https://doi.org/10.1002/cssc.202300135.
[68] H. Chen, N. Qiu, B. Wu, Z. Yang, S. Sun, Y. Wang, A new spinel high-entropy oxide (Mg0.2Ti0.2Zn0.2Cu0.2Fe0.2)3O4 with fast reaction kinetics and excellent stability as an anode material for lithium ion batteries, RSC Adv. 10 (2020) 9736–9744, https://doi.org/10.1039/d0ra00255k.
[69] J. Ma, B. Zhao, H. Xiang, F.Z. Dai, Y. Liu, R. Zhang, Y. Zhou, High-entropy spinel ferrites MFe2O4 (M = Mg, Mn, Fe, Co, Ni, Cu, Zn) with tunable electromagnetic properties and strong microwave absorption, J. Adv. Ceram. 11 (2022) 754–768, https://doi.org/10.1007/s40145-022-0569-3.
[70] C. Riley, N. Valdez, C.M. Smyth, R. Grant, B. Burnside, J.E. Park, S. Meserole, A. Benavidez, R. Craig, S. Porter, A. DeLaRiva, A. Datye, M. Rodriguez, S.S. Chou, Vacancy-driven stabilization of sub-stoichiometric aluminate spinel high entropy oxides, J. Phys. Chem. C. (2023), https://doi.org/10.1021/acs.jpcc.3c01499.
[71] A. Mohan, V. Hastak, A.S. Gandhi, Design and synthesis of a stable multicomponent equimolar high entropy oxide with spinel structure, Materialia 20 (2021), https://doi.org/10.1016/j.mtla.2021.101259.
[72] A.H. Phakatkar, M.T. Saray, M.G. Rasul, L.V. Sorokina, T.G. Ritter, T. Shokuhfar, R. Shahbazian-Yassar, Ultrafast synthesis of high entropy oxide nanoparticles by flame spray pyrolysis, Langmuir 37 (2021) 9059–9068, https://doi.org/10.1021/acs.langmuir.1c01105.
[73] A. Sarkar, B. Eggert, R. Witte, J. Lill, L. Velasco, Q. Wang, J. Sonar, K. Ollefs, S. S. Bhattacharya, R.A. Brand, H. Wende, F.M.F. de Groot, O. Clemens, H. Hahn, R. Kruk, Comprehensive investigation of crystallographic, spin-electronic and magnetic structure of (Co 0.2 Cr 0.2 Fe 0.2 Mn 0.2 Ni 0.2) 3 O 4: Unraveling the suppression of configuration entropy in high entropy oxides, Acta Mater. 226 (2022), 117581, https://doi.org/10.1016/j.actamat.2021.117581.